ON THE STRUCTURE OF TRI- AND TETRAHYDROXOLEAD(II) COMPLEX ANIONS

Stanislava ŠORALOVÁ[1] and Martin BREZA[2,*]

Department of Physical Chemistry, Slovak Technical University, SK-812 37 Bratislava, Slovakia; e-mail: [1] stanislava.soralova@stuba.sk, [2] martin.breza@stuba.sk

Received August 7, 2007
Accepted November 22, 2007

In the memory of Professor Ladislav Turi-Nagy (1947–2003).

Optimal geometries and corresponding electronic structures of various $[Pb(OH)_3]^-$ and $[Pb(OH)_4]^{2-}$ conformational isomers are investigated by the B3LYP and MP2 treatments. Unlike highly symmetric $[Pb(OH)_3]^-$ structure (C_3 symmetry), the most stable $[Pb(OH)_4]^{2-}$ conformational isomer has only C_2 symmetry. Hydrogen bonds exhibit a lower influence on the stereochemistry of lead(II) hydroxocomplexes in comparison with the steric effect of the Pb(II) lone electron pair. The picture of the Pb(II) lone electron pair cannot explain the lowered symmetry of isolated $[Pb(OH)_4]^{2-}$ complexes with four equivalent hydrogen bonds.
Keywords: Pb complexes; Lead; Lone electron pair; Hydroxocomplexes; Molecular structure; Geometry optimization; Hydrogen bonds; DFT calculations; Ab initio calculations.

Lead is known to be one of the most scattered heavy metals in the nature. Its compounds are known to be involved in biological processes where they usually act as poisons. Lead poisoning can involve either Pb(II) and Pb(IV) compounds, but all sources convert, in vivo or in aqueous media, to a number of Pb(II) compounds responsible for saturnism[1]. The mononuclear $[Pb(OH)_n]^{2-n}$ (aq) complexes are the only hydrolyzed species likely to be significant under typical environmental and biological conditions. Using various experimental techniques, the existence of only four species of this type ($n \leq 4$) has been confirmed[1]. The previously reported $[Pb(OH)_6]^{4-}$ seems to be an artifact of the potentiometric method used[2]. A variety of polynuclear complexes have been reported for high Pb concentrations in aqueous solutions but, except for $[Pb_3(OH)_4]^{2+}$, $[Pb_4(OH)_4]^{4+}$ and $[Pb_6(OH)_8]^{4+}$, they have not been well characterized[1,3–5].

Divalent lead, with its electronic configuration $[Xe]4f^{14}5d^{10}6s^2$, exhibits the so-called 'inert-pair effect'. This term refers to the resistance of the pair of outer electrons of Pb(II) to removal or to participation in covalent bond

Collect. Czech. Chem. Commun. 2008, Vol. 73, No. 1, pp. 59–72

doi:10.1135/cccc20080059

formation or hydrogen bonding. This has been explained as a relativistic effect causing the 6s orbital to contract, thereby increasing the energy required to remove or interact with the 6s lone pair of electrons. On the other hand, the d and f orbitals are destabilized because they expand radially as a result of shielding from nuclear attraction by the s and p electrons. The result is a stable, relatively inert outer lone pair of electrons which can cause a nonspherical charge distribution around the Pb(II) cation, i.e., the disposition of ligands around the cation results in an identifiable void (hemidirected lead coordination)[6–8]. Based on DFT electronic structure data, other authors[9,10] conclude that distorted Pb(II) structures are not the result of chemically inert, sterically active lone pairs but, instead, the result of asymmetric electron densities which rely on direct electronic interaction with the coordinated ligands. On the contrary, the 'lone pair' is the result of the lead–oxygen interaction.

Since for the tetracoordinated Pb(II) compounds only hemidirected structures have been found in the Cambridge Structure Database, ab initio molecular orbital calculations were performed to find any gas-phase holodirected complexes (i.e., without such void) with this coordination number[8]. A variety of Pb(II) complexes were optimized at the MP2 computational level, the LANL2DZ basis set was augmented with additional d functions for heavy atoms and the LANL2 pseudopotential was used for Pb atoms. This computational method incorporates the major relativistic effects (Darwin and mass–velocity terms) by fitting the atomic pseudopotential parameters to relativistic all-electron Hartree–Fock (HF) atomic wave functions. Molecular spin-orbit coupling is expected to be small for closed-shell species near their ground state and has not been considered. A hemidirected geometry has been found for $[Pb(OH)_4]^{2-}$ with Pb–O(1)/Pb–O(2) distances of 2.360 Å/2.197 Å and O(1)–Pb–O(3)/O(2)–Pb–O(4) angles of 144.7°/105.2°, respectively (see Chart 1 for atom notation). The energy difference between

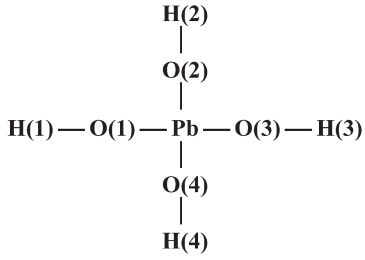

CHART 1
Atom notation in $[Pb(OH)_4]^{2-}$ complexes

optimized hemidirected (local minima) and holodirected (constrained tetrahedral) forms of this complex dianion is 28.6 kcal/mol (0.0456 a.u.); analogous values for other simple ligands are substantially lower[8]. Unfortunately, the MP2/LANL2DZp structure data of only a single $[Pb(OH)_4]^{2-}$ conformational isomer have been published in ref.[8] (moreover, only heavy atoms have been augmented by polarization functions). It must be mentioned that the MP2 and B3LYP geometry optimizations of neutral $Pb(OH)_4$ molecules resulted in S_4 symmetry in agreement with the infrared spectra measured in argon matrices[11].

The neutral $Pb(OH)_2$ molecule has been studied at DFT, MP2 and CCSD(T) levels of theory[11,12]. Its minimum energy structure has C_s symmetry with a weak intramolecular hydrogen bond. This is in agreement with the infrared spectra measured in argon matrices[11].

The $[Pb(OH)]^+$ complex cation has been studied by HF and DFT four-component relativistic calculations using an all-electron basis set[13]. It has been shown that fully relativistic calculations validate the use of scalar relativistic approaches within the framework of density functional theory. $[Pb(OH)]^+$ can be found bent or linear depending on the computational methodology used. When bent C_s structure is found, the barrier to inversion through the linear $C_{\infty v}$ structure is very low and can be overcome at sufficiently high temperature, making the molecule floppy. The neutral Pb(OH) molecule has been studied at DFT, MP2 and CCSD(T) levels of theory[12,14]. Eight stationary points have been found; four of them correspond to the stable PbOH and HPbO structures. The hydrogen inversion process in PbOH exhibits the so-called Renner–Teller effect with a rather low barrier, whereas the isomerization process PbOH → HPbO exhibits a rather high barrier. The minimum energy structure corresponds to the bent PbOH geometry (C_s symmetry)[14].

Various polynuclear complexes of the $[Pb_m(OH)_n]^{2m-n}$ and $[Pb_mO(OH)_n]^{2m-2-n}$ types have been studied at HF, DFT and MP2 levels of theory (for m = 2, 4, 6)[15–20] or using semiempirical AM1 treatment (m = 3, 4, 6)[21–24]. Direct Pb–Pb and O–O interactions are weakly antibonding in all the systems under study. The clusters are held together exclusively by relatively weak Pb–O bonds.

No quantum-chemical studies of $[Pb(OH)_3]^-$ have been found in the literature and the MP2/LANL2DZp study[8] of $[Pb(OH)_4]^{2-}$ assumes only a single conformational isomer of C_2 symmetry (without testing its stability). The aim of our study is to complete the geometry and electronic structure data of the above mentioned $[Pb(OH)_n]^{2-n}$ series and to shed more light on the influence of hydrogen bonds on their structures.

CALCULATIONS

Using Gaussian 03 program package[25], the optimal geometries of possible conformational isomers of $[Pb(OH)_3]^-$ and $[Pb(OH)_4]^{2-}$ complex anions are investigated within standard restricted B3LYP [26] and MP2 [27] (with the lowest orbital of every oxygen atom being kept frozen) treatments. Vibration analysis is used to verify the condition of potential energy surface minimum (no imaginary vibrations) and to evaluate the zero-point vibrational energy (ZPVE) correction. We have used various basis sets of different quality:

1) Dunning's correlation-consistent cc-pVDZ basis sets have been used for O and H atoms[28] whereas large-core LANL2 effective potential (78 electrons) and corresponding (3s,4p,1d)/[2s,3p,1d] basis set[29,30] with diffuse and polarization functions[30,31] have been used for Pb atoms (basis I) for comparison with our previous studies[16–24].

2) Dunning's correlation-consistent cc-pVTZ basis sets have been used for O and H atoms[30,32] whereas small-core CRENBL effective potential (68 electrons) and corresponding (3s,3p,4d) basis set[30,33] have been used for Pb atoms (basis II).

3) Alternatively, for $[Pb(OH)_3]^-$, cc-pVTZ basis set for O and H atoms[30,32], the large-core LANL2 effective potential and the corresponding (3s,4p,1d)/[2s,3p,1d] basis set[29,30] with diffuse and polarization functions[30,31] have been used for Pb atoms (basis III).

4) Alternatively, for $[Pb(OH)_3]^-$, cc-pVDZ basis set for O and H atoms[28] and small-core CRENBL effective potential with (3s,3p,4d) basis set[30,33] have been used for Pb atoms (basis IV).

Electron structure parameters have been evaluated in terms of Mulliken population analysis (gross atomic charges, overlap populations).

RESULTS AND DISCUSSION

As mentioned above, the geometry of lead(II) hydroxocomplexes may be understood as the result of effects of Pb lone pair and hydrogen bonds influences. Larger basis sets (such as cc-pVTZ) better describe hydrogen bonds. Analogously, the small-core effective potentials (such as CRENBL) can better describe the Pb lone pair effect than the large core ones (LANL2 uses only 2 electrons in the valence shell of Pb^{2+}). Thus the variation of basis sets and effective core potentials (ECPs) might help to better understand the role of the above influences. Due to practical reasons, we restricted this type of studies to $[Pb(OH)_3]^-$ only.

We started our study with six different conformations of $[Pb(OH)_3]^-$ but their geometry optimization leads to a single stable structure of C_3 symmetry (Fig. 1, Tables I and II). As expected, the optimized geometry is sensitive to the method (B3LYP or MP2) and especially to the basis sets as well as the effective core potentials (ECPs) used. Our results show that the greatest structure differences may be observed for Pb–O bonds and O–Pb–O angles the values of which are greater for small-core CRENBL effective potential (bases II and IV). Their increase causes hydrogen bond (O···H) elongation independent of the O and H basis sets used. Greater Pb–O–H bond angles are associated with larger basis sets. In spite of longer O···H distances, small O–Pb–O–H dihedral angles (i.e. nearly coplanar atoms) indicate that the hydrogen bonds may be preserved in all the cases mentioned. On the other hand, Mulliken overlap populations indicate that all the three hydrogen bonds are very weak or non-existent. Our results confirm a substantial dependence of Mulliken population analysis on the basis set/ECP used. Nevertheless, the overlap populations (Table II) indicate that O–H bonds are stronger than the Pb–O ones, in agreement with our previous studies on multinuclear lead(II) hydroxocomplexes[15–20].

Independent of the basis sets/ECPs used, Pb–O bonds are longer than in $Pb(OH)_2$ (2.022 Å/2.047 Å at the MP2 level[9] or 2.075 Å/2.105 Å at the B3LYP level[12] for the most stable conformational isomer) and $Pb(OH)^+$ species (1.895 Å at the B3LYP level[13]). The O–Pb–O angle (92.0° at the MP2 level[11] or 91.0° at the B3LYP level[12] for the most stable $Pb(OH)_2$ conformational isomer) and the Pb–O–H angle (112.1°/118.5° at the MP2 level[11] or 112.1°/116.9° at the B3LYP level[12] for the most stable $Pb(OH)_2$ conformational isomer, linear $Pb(OH)^+$ at the B3LYP level[13]) exhibit the reverse trend.

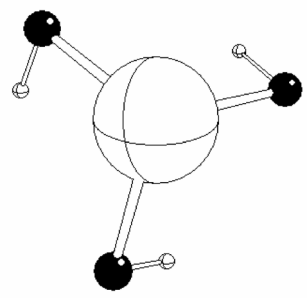

FIG. 1
Geometry of $[Pb(OH)_3]^-$, model A (C_3 symmetry)

The geometry optimization of nine starting conformations of $[Pb(OH)_4]^{2-}$ leads to four stable structures of low symmetry in basis I (B1–B4 models) but the last one (B4) has not been found in larger basis II (Fig. 2, Tables I and III–VI). This confirms our above mentioned thesis on the main effect of

TABLE I
Total energy, without (E_{tot}) and with ZPVE correction (E_{tot} + ZPVE), of the systems under study in various basis sets and at various levels of theory

Compound	Model	Symmetry group	Basis	Method	E_{tot} a.u.	E_{tot} + ZPVE a.u.
$[Pb(OH)_3]^-$	A	C_3	I	B3LYP	–231.05837	–231.02101
				MP2	–230.41891	–230.38055
			II	B3LYP	–288.97518	–288.93902
				MP2	–287.22247	–287.18541
			III	B3LYP	–231.16472	–231.12724
				MP2	–230.69282	–230.65479
			IV	B3LYP	–288.88003	–288.84401
				MP2	–286.95888	–286.92171
$[Pb(OH)_4]^{2-}$	B1	C_1	I	B3LYP	–306.73872	–306.68871
				MP2	–305.89716	–305.84554
			II	B3LYP	–364.71150	–364.66413
				MP2	–362.81429	–362.76543
	B2	C_2	I	B3LYP	–306.74434	–306.69278
				MP2	–305.90236	–305.84943
			II	B3LYP	–364.71339	–364.66496
				MP2	–362.81625	–362.76644
	B3	C_1	I	B3LYP	–306.73527	–306.68520
				MP2	–305.89290	–305.84128
			II	B3LYP	–364.70958	–364.66252
				MP2	–362.81163	–362.76273
	B4	C_1	I	B3LYP	–306.72842	–306.68004
				MP2	–305.88465	–305.83441

Pb lone pair in stereochemistry of our systems which may be modified by hydrogen bonds.

Our structure data (such as small O–Pb–O–H dihedral angles) indicate that B1, B2 and B3 models have four hydrogen bonds whereas B4 only two (and this might be the reason why it has not been found in the basis II). Nevertheless, Mulliken overlap populations indicate that only few of these hydrogen bonds might be important. Only the most stable B2 model structure has C_2 symmetry axis, the remaining stable structures are asymmetric. The symmetric hydrogen bonds in the B2 model are equivalent and cannot be the source of symmetry decrease. Moreover, the optimal geometry of $[PbF_4]^{2-}$ without any hydrogen bonds is of C_{2v} symmetry as well[8] (not C_{4v}). Consequently, the symmetry decrease is ascribed to the Pb lone electron

TABLE II
Geometry and electronic structure data for the optimal geometry of $[Pb(OH)_3]^-$, model A (C_3 symmetry), obtained with various basis sets and at various levels of theory

Structure data	I		II		III		IV	
	B3LYP	MP2	B3LYP	MP2	B3LYP	MP2	B3LYP	MP2
Bond lengths, Å								
Pb–O(1)	2.120	2.118	2.314	2.279	2.123	2.144	2.297	2.275
O(1)–H(1)	0.974	0.973	0.963	0.965	0.964	0.964	0.972	0.972
O(1)···H(2)	2.577	2.553	3.109	2.927	2.674	2.613	3.031	2.890
Bond angles, °								
O(1)–Pb–O(2)	90.6	90.6	96.1	93.9	92.0	91.5	95.2	93.7
Pb–O(1)–H(1)	99.4	97.9	104.0	100.3	102.2	100.1	102.4	99.0
Dihedral angles, °								
O(2)–Pb–O(1)–H(1)	89.0	88.0	91.5	90.5	90.0	88.8	88.7	89.5
O(3)–Pb–O(1)–H(1)	–1.6	–2.7	–5.4	–3.8	–2.2	–2.8	–7.0	–4.5
Atomic charges								
Pb	0.560	0.647	0.598	0.560	0.863	0.937	0.226	0.200
O(1)	–0.623	–0.661	–0.718	–0.729	–0.817	–0.856	–0.528	–0.534
H(1)	0.103	0.112	0.185	0.209	0.197	0.211	0.119	0.134
Overlap populations								
Pb–O(1)	0.215	0.213	0.207	0.201	0.158	0.155	0.276	0.272
O(1)–H(1)	0.290	0.285	0.269	0.224	0.255	0.225	0.302	0.295
O(1)···H(2)	0.011	0.010	0.001	0.002	0.011	0.010	–0.002	–0.004

pair despite the existence of high-symmetric $[Pb(OH)_3]^-$ (see Table II) and other high-symmetric lead(II) halocomplexes[8] (such as tetrahedral $[PbX_4]^{2-}$, X = Cl, Br, I). According to the author's opinion, this explanation is insufficient and the reason for the mentioned symmetry decrease is more complex (maybe the pseudo-Jahn–Teller effect).

The energy differences between stable conformational isomers (Table I) are of the same order as the energy difference between optimized hemidirected and holodirected $[Pb(OH)_4]^{2-}$ structures in ref.[8]. This confirms the importance of hydrogen bonding in hemidirected lead(II) coordination. Similarly as above, the greatest structure differences between the optimal structures obtained in both bases may be observed for the Pb–O bond and O–Pb–O angles whose values are greater for basis II. The same relation holds for Pb–O–H bond angles. In general, Pb–O bonds are longer in $[Pb(OH)_4]^{2-}$ than in $[Pb(OH)_3]^-$ (due to the more negative ion charge and the higher coordination number) whereas the reverse relation holds for Pb–O–H and most O–Pb–O angles (except the trans O(1)–Pb–O(3) and O(2)–Pb–O(4) ones, which are missing in $[Pb(OH)_3]^-$). The differences between ref.[8] and our data on the B2 model structure in basis I (Table IV) may be ascribed to

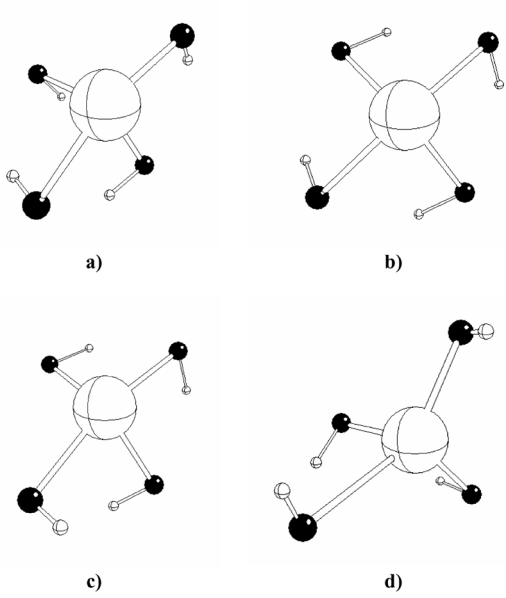

FIG. 2
Geometry of $[Pb(OH)_4]^{2-}$; a model B1 (C_1 symmetry), b model B2 (C_2 symmetry), c model B3 (C_1 symmetry) and d model B4 (C_1 symmetry)

TABLE III

Geometry and electronic structure data of the optimal geometry of $[Pb(OH)_4]^{2-}$, model B1 (C_1 symmetry), obtained with various basis sets and at various levels of theory (see Chart 1 for atom numbering)

Structural data	I		II	
	B3LYP	MP2	B3LYP	MP2
Bond lengths, Å				
Pb–O(1)/Pb–O(3)	2.141/2.190	2.142/2.185	2.356/2.407	2.304/2.359
Pb–O(2)/Pb–O(4)	2.549/2.257	2.488/2.252	2.586/2.511	2.578/2.461
O(1)–H(1)/O(3)–H(3)	0.993/0.977	0.989/0.975	0.968/0.964	0.973/0.966
O(2)–H(2)/O(4)–H(4)	0.977/0.974	0.974/0.973	0.964	0.964
O(1)···H(4)/O(3)···H(2)	2.466/2.300	2.422/2.286	2.852/3.126	2.694/2.962
O(2)···H(1)/O(1)···H(3)	1.846/2.429	1.852/2.422	2.371/2.962	2.157/2.763
Bond angles, °				
O(1)–Pb–O(3)/O(2)–Pb–O(4)	87.0/152.7	87.6/153.2	92.2/157.6	90.1/155.5
O(1)–Pb–O(2)/O(3)–Pb–O(4)	69.3/95.2	70.6/93.9	77.2/103.2	73.9/102.1
O(1)–Pb–O(4)/O(3)–Pb–O(2)	84.0/78.2	83.4/79.0	86.4/92.8	85.3/90.9
Pb–O(1)–H(1)/Pb–O(3)–H(3)	88.3/92.5	86.6/90.9	90.4/96.3	87.4/92.9
Pb–O(2)–H(2)/Pb–O(4)–H(4)	82.4/96.6	83.2/94.7	94.1/96.9	89.8/93.6
Dihedral angles, °				
O(3)–Pb–O(1)–H(1)/O(1)–Pb–O(3)–H(3)	–79.5/–9.1	–79.9/–8.6	–91.3/–8.1	–90.7/–6.7
O(2)–Pb–O(1)–H(1)/O(4)–Pb–O(3)–H(3)	–1.0/74.6	–0.7/74.6	1.1/78.8	0.2/78.5
O(4)–Pb–O(1)–H(1)/O(2)–Pb–O(3)–H(3)	–175.1/–78.6	–174.1/–79.3	165.7/–85.4	167.1/–80.6
O(1)–Pb–O(2)–H(2)/O(3)–Pb–O(4)–H(4)	–96.5/–72.4	–94.9/–70.1	–93.7/–84.2	–93.2/–81.2
O(3)–Pb–O(2)–H(2)/O(1)–Pb–O(4)–H(4)	–5.3/14.0	–3.6/17.0	–2.1/7.3	–3.4/7.8
O(4)–Pb–O(2)–H(2)/O(2)–Pb–O(4)–H(4)	–83.6/1.8	–80.2/3.1	–137.9/50.2	167.1/139.5
Atomic charges				
Pb	0.261	0.439	0.469	0.439
O(1)/O(3)	–0.667/–	–0.708/–0.674	–0.757/–0.753	–0.576/–0.571
O(2)/O(4)	–0.644/–	–0.701/–0.690	–0.803/–0.790	–0.837/–0.809
H(1)/H(3)	0.089/0.079	0.093/0.084	0.167/0.164	0.198/0.193
H(2)/H(4)	0.064/0.086	0.068/0.088	0.150/0.153	0.176/0.178
Overlap populations				
Pb–O(1)/Pb–O(3)	0.209/0.200	0.210/0.201	0.202/0.197	0.200/0.196
Pb–O(2)/Pb–O(4)	0.145/0.208	0.145/0.202	0.173/0.202	0.160/0.196
O(1)–H(1)/O(3)–H(3)	0.266/0.273	0.266/0.267	0.219/0.258	0.186/0.217
O(2)–H(2)/O(4)–H(4)	0.277/0.280	0.272/0.272	0.258/0.261	0.222/0.220
O(1)···H(4)/O(3)···H(2)	0.009/0.030	0.008/0.027	0.003/0.000	0.003/0.000
O(2)···H(1)/O(1)···H(3)	0.084/0.022	0.079/0.020	0.034/0.006	0.047/0.009

TABLE IV

Geometry and electronic structure data of the optimal geometry of $[Pb(OH)_4]^{2-}$, model B2 (C_2 symmetry), obtained with various basis sets and at various levels of theory and their comparison with structure data in ref.[8] (see Chart 1 for atom numbering)

Structural data	Ref.[8]	I		II	
	MP2	B3LYP	MP2	B3LYP	MP2
Bond lengths, Å					
Pb–O(1)/Pb–O(3)	2.350	2.314	2.312	2.507	2.470
Pb–O(2)/Pb–O(4)	2.197	2.211	2.193	2.382	2.334
O(1)–H(1)/O(3)–H(3)	0.973	0.977	0.975	0.964	0.965
O(2)–H(2)/O(4)–H(4)	0.976	0.982	0.980	0.966	0.969
O(1)···H(2)/O(3)···H(4)	2.215	2.022	2.014	2.536	2.358
O(2)···H(3)/O(4)···H(1)	2.381	2.155	2.167	2.785	2.593
Bond angles, °					
O(1)–Pb–O(3)/O(2)–Pb–O(4)	144.7/ 105.2	131.3/ 109.8	135.2/ 107.1	157.5/ 108.1	151.2/ 105.0
O(1)–Pb–O(2)/O(3)–Pb–O(4)	78.3	75.1	75.6	81.3	79.3
O(1)–Pb–O(4)/O(3)–Pb–O(2)	80.5	77.5	78.2	85.5	83.3
Pb–O(1)–H(1)/Pb–O(3)–H(3)	93.7	87.4	86.7	94.4	90.5
Pb–O(2)–H(2)/Pb–O(4)–H(4)	93.2	88.0	87.0	91.8	88.7
Dihedral angles, °					
O(3)–Pb–O(1)–H(1)/O(1)–Pb–O(3)–H(3)	–46.0	–48.9	–46.3	–49.5	–47.7
O(2)–Pb–O(1)–H(1)/O(4)–Pb–O(3)–H(3)	–74.7	–106.7	–102.4	–79.5	–77.0
O(4)–Pb–O(1)–H(1)/O(2)–Pb–O(3)–H(3)	7.7	8.0	8.9	4.7	5.2
O(1)–Pb–O(2)–H(2)/O(3)–Pb–O(4)–H(4)	2.9	4.6	4.1	2.9	3.0
O(3)–Pb–O(2)–H(2)/O(1)–Pb–O(4)–H(4)	–149.7	–134.8	–139.2	–158.9	–154.0
O(4)–Pb–O(2)–H(2)/O(2)–Pb–O(4)–H(4)	–100.2	–65.9	–68.4	–79.5	–77.0
Atomic charges					
Pb	–	0.204	0.386	0.464	0.434
O(1)/O(3)	–	–0.641	–0.693	–0.803	–0.831
O(2)/O(4)	–	–0.641	–0.688	–0.753	–0.765
H(1)/H(3)	–	0.092	0.095	0.161	0.188
H(2)/H(4)	–	0.088	0.092	0.163	0.191
Overlap populations					
Pb–O(1)/Pb–O(3)	–	0.187	0.182	0.197	0.186
Pb–O(2)/Pb–O(4)	–	0.208	0.209	0.203	0.204
O(1)–H(1)/O(3)–H(3)	–	0.282	0.277	0.261	0.218
O(2)–H(2)/O(4)–H(4)	–	0.276	0.273	0.229	0.195
O(1)···H(2)/O(3)···H(4)	–	0.054	0.051	0.016	0.022
O(2)···H(3)/O(4)···H(1)	–	0.032	0.025	0.004	0.005

TABLE V

Geometry and electronic structure data of the optimal geometry of $[Pb(OH)_4]^{2-}$, model B3 (C_1 symmetry), obtained with various basis sets and at various levels of theory (see Chart 1 for atom numbering)

Structural data	I		II	
	B3LYP	MP2	B3LYP	MP2
Bond lengths, Å				
Pb–O(1)/Pb–O(3)	2.446/2.329	2.409/2.321	2.564/2.514	2.523/2.481
Pb–O(2)/Pb–O(4)	2.193/2.164	2.189/2.157	2.395/2.381	2.344/2.323
O(1)–H(1)/O(3)–H(3)	0.975/0.976	0.973/0.974	0.964	0.964
O(2)–H(2)/O(4)–H(4)	0.982/0.983	0.979/0.980	0.964/0.966	0.967/0.970
O(1)···H(2)/O(3)···H(4)	2.030/2.026	2.043/2.025	2.747/2.616	2.475/2.298
O(2)···H(3)/O(4)···H(1)	2.242/2.684	2.223/2.598	2.820/4.301	2.627/4.229
Bond angles, °				
O(1)–Pb–O(3)/O(2)–Pb–O(4)	144.9/104.5	145.7/103.9	167.1/103.8	159.5/104.2
O(1)–Pb–O(2)/O(3)–Pb–O(4)	72.9/76.1	73.8/76.6	81.6/83.5	79.1/78.4
O(1)–Pb–O(4)/O(3)–Pb–O(2)	90.5/79.2	89.4/79.3	98.8/85.5	95.3/83.5
Pb–O(1)–H(1)/Pb–O(3)–H(3)	91.9/88.6	90.1/87.4	94.6/95.5	91.7/91.0
Pb–O(2)–H(2)/Pb–O(4)–H(4)	89.4/87.9	88.3/86.9	96.3/91.3	91.4/87.2
Dihedral angles, °				
O(3)–Pb–O(1)–H(1)/O(1)–Pb–O(3)–H(3)	107.2/–28.8	102.7/–28.9	32.4/6.1	82.0/–23.9
O(2)–Pb–O(1)–H(1)/O(4)–Pb–O(3)–H(3)	68.3/–99.2	62.9/–97.5	28.8/–94.8	49.1/–97.4
O(4)–Pb–O(1)–H(1)/O(2)–Pb–O(3)–H(3)	173.4/8.9	167.6/9.8	131.6/9.6	152.6/8.6
O(1)–Pb–O(2)–H(2)/O(3)–Pb–O(4)–H(4)	13.9/2.2	15.9/2.4	26.9/1.4	19.0/1.0
O(3)–Pb–O(2)–H(2)/O(1)–Pb–O(4)–H(4)	–144.5/–145.0	–142.6/–145.9	–152.3/–165.7	–149.9/–159.3
O(4)–Pb–O(2)–H(2)/O(2)–Pb–O(4)–H(4)	–72.1/–72.5	–69.4/–72.7	–70.1/–82.3	–73.7/–79.2
Atomic charges				
Pb	0.231	0.413	0.469	0.439
O(1)/O(3)	–0.618/–0.648	–0.673/–0.701	–0.786/–0.809	–0.798/–0.839
O(2)/O(4)	–0.644/–0.630	–0.691/–0.675	–0.752/–0.740	–0.768/–0.746
H(1)/H(3)	0.057/0.089	0.062/0.091	0.122/0.160	0.136/0.189
H(2)/H(4)	0.080/0.083	0.085/0.088	0.151/0.150	0.181/0.177
Overlap populations				
Pb–O(1)/Pb–O(3)	0.144/0.181	0.143/0.179	0.184/0.189	0.178/0.176
Pb–O(2)/Pb–O(4)	0.205/0.238	0.202/0.236	0.193/0.205	0.199/0.219
O(1)–H(1)/O(3)–H(3)	0.270/0.284	0.263/0.276	0.246/0.259	0.194/0.220
O(2)–H(2)/O(4)–H(4)	0.272/0.273	0.269/0.271	0.254/0.222	0.211/0.182
O(1)···H(2)/O(3)···H(4)	0.060/0.054	0.053/0.049	0.009/0.017	0.175/0.220
O(2)···H(3)/O(4)···H(1)	0.023/0.008	0.020/0.010	0.004/0.000	0.004/0.000

TABLE VI
Geometry and electronic structure data of the optimal geometry of $[Pb(OH)_4]^{2-}$, model B4 (C_1 symmetry), obtained at various levels of theory (see Chart 1 for atom numbering)

Structural data	I	
	B3LYP	MP2
Bond lengths, Å		
Pb–O(1)/Pb–O(3)	2.171/2.990	2.280/2.695
Pb–O(2)/Pb–O(4)	2.251/2.093	2.163/2.113
O(1)–H(1)/O(3)–H(3)	0.976/0.976	0.971/0.973
O(2)–H(2)/O(4)–H(4)	0.974/1.009	0.975/0.996
O(3)···H(4)	1.730	1.789
O(4)···H(2)	3.924	2.433
Bond angles, °		
O(1)–Pb–O(3)/O(2)–Pb–O(4)	106.1/93.7	151.2/88.6
O(1)–Pb–O(2)/O(3)–Pb–O(4)	99.6/60.5	99.2/66.6
O(1)–Pb–O(4)/O(3)–Pb–O(2)	89.3/142.6	91.6/98.8
Pb–O(1)–H(1)/Pb–O(3)–H(3)	94.5/77.0	90.6/81.8
Pb–O(2)–H(2)/Pb–O(4)–H(4)	95.2/92.2	92.0/87.6
Dihedral angles, °		
O(3)–Pb–O(1)–H(1)/O(1)–Pb–O(3)–H(3)	–66.4/173.3	121.7/–45.5
O(2)–Pb–O(1)–H(1)/O(4)–Pb–O(3)–H(3)	86.1/93.6	–110.3/–89.0
O(4)–Pb–O(1)–H(1)/O(2)–Pb–O(3)–H(3)	–7.5/41.8	160.9/–173.6
O(1)–Pb–O(2)–H(2)/O(3)–Pb–O(4)–H(4)	101.0/4.4	–85.0/–4.5
O(3)–Pb–O(2)–H(2)/O(1)–Pb–O(4)–H(4)	–125.8/–104.6	72.4/–165.1
O(4)–Pb–O(2)–H(2)/O(2)–Pb–O(4)–H(4)	–169.1/155.9	6.3/95.7
Atomic charges		
Pb	0.222	0.390
O(1)/O(3)	–0.624/–0.639	–0.660/–0.684
O(2)/O(4)	–0.609/–0.674	–0.662/–0.703
H(1)/H(3)	0.096/0.044	0.076/0.045
H(2)/H(4)	0.074/0.110	0.099/0.098
Overlap populations		
Pb–O(1)/Pb–O(3)	0.220/0.102	0.164/0.114
Pb–O(2)/Pb–O(4)	0.173/0.233	0.229/0.231
O(1)–H(1)/O(3)–H(3)	0.278/0.271	0.274/0.259
O(2)–H(2)/O(4)–H(4)	0.283/0.255	0.269/0.259
O(3)···H(4)	0.112	0.092
O(4)···H(2)	0.000	0.017

missing polarization functions on hydrogen atoms in ref.[6], which causes a weakening of the hydrogen bonds. This is an indirect proof of the importance of weak interactions in this type of compounds.

CONCLUSIONS

Despite the significant basis set dependence of Mulliken population analysis it may be concluded that the Pb–O bonds in $[Pb(OH)_4]^{2-}$ are less polar and weaker than in $[Pb(OH)_3]^-$ (see atomic charges and overlap populations in Tables II–V). Similarly as above, Pb–O bonds are weaker than O–H bonds in agreement with our previous studies of polynuclear lead(II) hydroxocomplexes[15–20]. Due to steric reasons, the possible hydrogen bonds in $[Pb(OH)_3]^-$ are weaker than in $[Pb(OH)_4]^{2-}$.

The agreement between B3LYP and MP2 data is fairly good (except for the B4 model). In general, the MP2 treatment seems to be more reliable due to better accounting for weak interactions.

Finally it can be concluded that hydrogen bonds exhibit a significant influence on the stereochemistry of lead(II) hydroxocomplexes and are able to modify the steric effect of the Pb(II) lone electron pair. Both these effects might explain the hemidirected lead coordination observed in real systems[8]. On the other hand, the picture of the Pb lone electron pair cannot explain the symmetry decrease in isolated $[Pb(OH)_4]^{2-}$ complexes. Additional experimental as well as theoretical studies are desirable to explain this problem in more detail.

The work reported in this paper has been funded by the Slovak Grant Agency VEGA, project No. 1/3566/06.

REFERENCES AND NOTES

1. Perera W. N., Hefter G., Sipos P. M.: *Inorg. Chem.* **2001**, *40*, 3974; and references therein.
2. Ferri D., Salvatore F., Vasca E.: *Ann. Chim.* **1989**, *79*, 1.
3. Johansson G., Olin A.: *Acta Chem. Scand.* **1968**, *22*, 3197.
4. Olin A., Söderquist R.: *Acta Chem. Scand.* **1972**, *26*, 3505.
5. Grimes S. M., Johnston S. R., Abrahams I.: *J. Chem. Soc., Dalton Trans.* **1995**, 2081.
6. Schwerdtfeger P., Heath G. A., Dolg M., Bennett M. A.: *J. Am. Chem. Soc.* **1992**, *114*, 7518.
7. Seth M., Faegri K., Schwerdtfeger P.: *Angew. Chem. Int. Ed.* **1998**, *37*, 2493.
8. Shimoni-Livny L., Glusker J. P., Bock Ch. W.: *Inorg. Chem.* **1998**, *37*, 1853; and references therein.
9. Watson G. W., Parker S. C., Kresse G.: *Phys. Rev. B* **1999**, *59*, 8481.
10. Walsh A., Watson G. W.: *J. Solid State Chem.* **2005**, *178*, 1422.

11. Wang X. F., Andrews L.: *J. Phys. Chem. A* **2005**, *109*, 9013.
12. Benjelloun A. T., Daoudi A., Chermette H.: *Mol. Phys.* **2005**, *103*, 317.
13. Gourlaouen C., Piquemal J. P., Parisel O.: *J. Chem. Phys.* **2006**, *124*, 174311.
14. Benjelloun A. T., Daoudi A., Chermette H.: *J. Chem. Phys.* **2004**, *121*, 7207.
15. Jensen J. O.: *J. Mol. Struct. (THEOCHEM)* **2002**, *587*, 111.
16. Breza M., Biskupič S., Manová A.: *Polyhedron* **2003**, *22*, 2863.
17. Breza M., Biskupič S.: *Collect. Czech. Chem. Commun.* **2003**, *68*, 2377.
18. Breza M., Biskupič S.: *Collect. Czech. Chem. Commun.* **2004**, *69*, 2045.
19. Breza M., Biskupič S.: *Collect. Czech. Chem. Commun.* **2004**, *69*, 2055.
20. Breza M., Manová A.: *J. Mol. Struct. (THEOCHEM)* **2006**, *765*, 121.
21. Breza M., Manová A.: *Collect. Czech. Chem. Commun.* **1995**, *60*, 527.
22. Breza M., Manová A.: *Polyhedron* **1999**, *18*, 2085.
23. Breza M., Manová A.: *Collect. Czech. Chem. Commun.* **1999**, *64*, 1269.
24. Breza M., Manová A.: *Collect. Czech. Chem. Commun.* **2002**, *67*, 219.
25. Frisch M. J., Trucks G. W., Schlegel H. B., Scuseria G. E., Robb M. A., Cheeseman J. R., Montgomery J. A., Jr., Vreven T., Kudin K. N., Burant J. C., Millam J. M., Iyengar S. S., Tomasi J., Barone V., Mennucci B., Cossi M., Scalmani G., Rega N., Petersson G. A., Nakatsuji H., Hada M., Ehara M., Toyota K., Fukuda R., Hasegawa J., Ishida M., Nakajima T., Honda Y., Kitao O., Nakai H., Klene M., Li X., Knox J. E., Hratchian H. P., Cross J. B., Adamo C., Jaramillo J., Gomperts R., Stratmann R. E., Yazyev O., Austin A. J., Cammi R., Pomelli C., Ochterski J. W., Ayala P. Y., Morokuma K., Voth G. A., Salvador P., Dannenberg J. J., Zakrzewski V. G., Dapprich S., Daniels A. D., Strain M. C., Farkas O., Malick D. K., Rabuck A. D., Raghavachari K., Foresman J. B., Ortiz J. V., Cui Q., Baboul A. G., Clifford S., Cioslowski J., Stefanov B. B., Liu G., Liashenko A., Piskorz P., Komaromi I., Martin R. L., Fox D. J., Keith T., Al-Laham M. A., Peng C. Y., Nanayakkara A., Challacombe M., Gill P. M. W., Johnson B., Chen W., Wong M. W., Gonzalez C., Pople J. A.: *Gaussian 03*, Revision C.1. Gaussian, Inc., Pittsburgh (PA) 2003.
26. Becke A. D.: *J. Chem. Phys.* **1993**, *98*, 5648.
27. Møller C., Plesset M. S.: *Phys. Rev.* **1934**, *46*, 618.
28. Woon D. E., Dunning T. H., Jr.: *J. Chem. Phys.* **1993**, *98*, 1358.
29. Hay P. J., Wadt W. R.: *J. Chem. Phys.* **1985**, *82*, 299.
30. Available from: http://www.emsl.pnl.gov/forms/basisform.html. Basis sets were obtained from the Extensible Computational Chemistry Environment Basis Set Database, Version 02/25/04, as developed and distributed by the Molecular Science Computing Facility, Environmental and Molecular Sciences Laboratory which is a part of the Pacific Northwest Laboratory, P.O. Box 999, Richland, Washington 99352, U.S.A., and funded by the U.S. Department of Energy. The Pacific Northwest Laboratory is a multiprogram laboratory operated by the Battelle Memorial Institute for the U.S. Department of Energy under contract DE-AC06-76RLO 1830.
31. Check C. E., Faust T. O., Bailey J. M., Wright B. J., Gilbert T. M., Sunderlin L. S.: *J. Phys. Chem. A* **2001**, *105*, 8111.
32. Dunning T. H.: *J. Chem. Phys.* **1989**, *90*, 1007.
33. Ermler W. C., Ross R. B., Christiansen P. A.: *Int. J. Quantum Chem.* **1991**, *40*, 829.